International Research Journal of Engineering and Technology (IRJET) e-ISSN: 2395-0056
Volume: 04 Issue: 08 | Aug -2017 www.irjet.net p-ISSN: 2395-0072

Artificial Neural Network based monitoring of Weld Quality in Pulsed Metal Inert Gas Welding using Wavelet Packets of Current Signal

Mr. Shashank Srivastava and Mr.Samuel Debbarma

[1] B.Tech 2012 Batch ,Department of Mechanical Engineering,Beant College of Engineering and Technology Gurdaspur Punjab India, H.no1 Puspa Niketan Kali Bari marg Cantt. Road Lucknow UP 226001Phone:
[2]M.Tech Scholar, Department of Mechanical Engineering, NIT Silchar, India,Hno.66 By Lane3,Ujan Abhoynagar Agartala ,Tripura West India

---***---

Abstract - *Pulsed metal inert gas welding (P-MIGW) is often used to improve weld quality using an advanced spray metal transfer with less heat input to the weld. It is a nonlinear process with various uncertainties like contamination. Thus, the necessity for online welding process monitoring has increased in modern manufacturing environment. Though, statistical regression methods are widely used to develop mathematical models in arc welding, it found to be inadequate to predict some specific weld quality features like joint strength. So, various intelligent tools like soft computing techniques are developed with better predictability. Different sensor based features may also be useful to improve the process monitoring. This paper addresses different statistical features as well as time-frequency wavelet packet coefficients of sensors' signals like voltage, current for the prediction of weld quality features in P-MIGW. The voltage and welding current signals have been acquired during welding experiments as per response surface design of experiment technique. Initially, a comparison has been made between regression models and back propagation neural network (BPNN) models for weld quality characteristics as a function of process parameters like peak voltage, pulse frequency, welding speed, torch angle etc. The mathematical regression models were found to be inadequate. Therefore, BPNN model has been retrained using different sensor based features to improve in weld quality prediction capability. Wavelet packets of welding current were found to be an important indicator of butt joint strength.*

Key Words: Weld Joint strength, hardness variation, Pulse parameters, Arc power, Wavelet packet coefficient.

1. INTRODUCTION

Pulsed metal inert gas welding (P-MIGW) is often used in today's manufacturing industries because of uniform metal transfer without any spatter at realistic cost than constant voltage arc welding processes. It is a superior spray metal transfer with reduced heat input to the weld. It is a variation of constant voltage arc welding which engage cycling of the arc voltage from a peak value to a root value at a particular frequency [1]. Current pulsing is applied to obtain uniform finer grain in fusion zone (FZ) which may produce high joint strength because of uniform hardness in FZ and heat affected zone (HAZ) interface. The weld quality is the best for one droplet of molten metal transfer at the end of wire electrode per one pulse in pulsed gas metal arc welding (PGMAW) [2]. The weld quality characteristics primarily depend on bead geometry [3] and weld microstructure [4], which in turn indicate the joint strength and welded plate distortions. These bead features are affected by the metal transfer modes and arc stability in GMAW. Therefore, it is necessary to establish a relation between weld quality features with the process parameters. The conventional mathematical regression tools like response surface methodology (RSM) focus mainly on the mean of the performance characteristic, whereas the Taguchi method considers the variance to develop the model in arc welding. Various numerical and analytical thermal models like finite element method also found to be useful to build up the weld distortion model. However, arc welding processes, being highly dynamic and nonlinear with various types of uncertainties like environmental conditions, it is really difficult to design reliable welds. This multivariate environment indicates the necessity for an intelligent system which can characterize and monitor the process in a better way.

The soft computing tools like artificial neural network (ANN) provide an alternative approach for predictive learning and modelling of weld quality without any mathematical model. These evolutionary algorithms consider the uncertainty features of the welding processes, which may not be expressed by mathematical equations. Thus, they are better compared to conventional statistical and analytical techniques. These tools can handle a large number of data to generate the model and optimize it with a short time span. These tools are also adaptable for incremental learning, enabling the models to be improved incrementally as new data become available. In recent years, weld quality can be monitored in real time with the application of adaptive sensor integrated control systems [5-6].

In the present work, two major weld quality features namely, joint strength (σ_t) and hardness variation in the FZ-HAZ interface ($\Delta H_{w\text{-}h}$) have been modelled using ANN as well as RSM to improve process monitoring for achieve a desired weld bead in P-MIGW. The models are compared and validated by using the data from validation experiments. The welding torch angle (α_t), welding speed (S), and wire feed rate (F) along with three major pulse parameters, such as peak voltage (V_p), pulse frequency (f_p) and pulse on-time (t_p) were considered for model development. Various time domain statistical features as well as time-frequency wavelet features of current and voltage signals have also been used in ANN models for further improvement of the predictions.

23] investigated the physical laws for the thermo-piezoelectric materials. Chandrasekharaiah [24] generalized Mindlin's theory of thermo-piezoelectricity to account for the finite speed of propagation of thermal disturbances on the basis of the first and the second thermodynamics laws. He et al. respectively investigated a two-dimensional generalized thermo-piezoelectric problem subjected to a thermal shock by hybrid Laplace transform-finite element method based on G-L theory [25] and a one-dimensional generalized thermo-piezoelectric problem subjected to a moving heat source by Laplace transform and its numerical inversion in the context of L-S theory [26]. So far, there are few works devoting to the investigation of the dynamic response for piezoelectric-thermo elastic problems in the context of fractional order theory of thermoelasticity.

In present work, we focus on investigating the dynamic response of a generalized piezoelectric-thermo elastic problem subjected to a moving heat source under the fractional order theory of thermoelasticity. The problem is solved by means of Laplace transform. The variations of the considered variables are obtained and illustrated graphically.

1.1. Experimental Procedure

In this work, a constant voltage P-MIGW machine (FRONIOUS make) was used. The experiments were carried out on 6 mm mild steel plates using same type 1.2 mm diameter electrode wire. Pure argon was used as the shielding gas. Initially, fifty three butt welding experiments have been carried out using half fractional central composite response surface methodology. The butt weld joints made of one pair of plates were tack welded at the two ends before final welding. A Hall-effect current sensor (LEM, model LT 500S) and voltage sensor were used to acquire the actual process behaviour. The signals were acquired using one A/D cards (National Instruments, USB-6210) to an Intel Pentium-4 PCs using LabVIEW 7.1 data acquisition interface at a sampling frequency of 40 kHz. The schematic representation of the experimental set-up is shown in Figure 1.

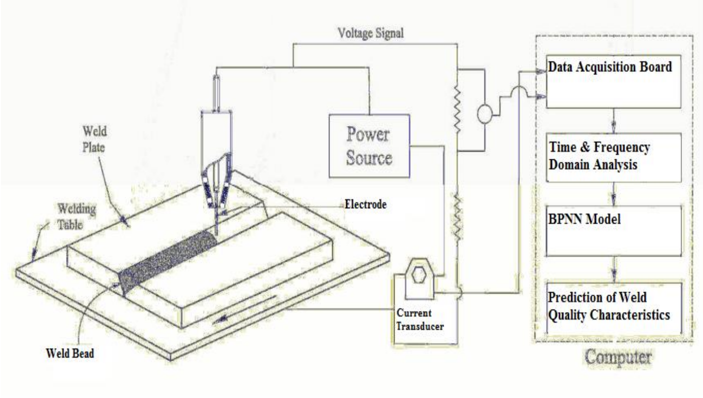

Fig. 1. Schematic diagram of experimental set-up

The butt welded joint specimens have been prepared to measure hardness variation and tensile test according to ASTM standard. The tensile characteristics have been measured by universal tensile testing machine (INSTRON, 8862) with attached software (Instron Wave Matrix). The weld bead was cut crosswise by an abrasive cutter (Buehler Delta Abrasimet, 10-2155). The weld fusion zone and HAZ have been identified under microscopes after cutting, grinding and polishing (using Buehler Ecomet® 3000), and etching with 2% nital solution. The micro-hardness was measured with the help of micro-hardness tester (UHL VMHT, VMH 001) at 500 gf in various weld zones. The butt weld joint samples have been prepared for the tensile test according to ASTM (E 8) standard. The hardness variation at the FZ-HAW interface was considered with the ultimate joint tensile strength as these parameters primarily indicate the butt weld joint quality.

The acquired voltage and current signals were post-processed in the time domain to obtain their root mean square (RMS) values V_{rms} and I_{rms}, respectively. Various time domain statistical values like mean, RMS, standard deviation and kurtosis of sensors' signals were found to be correlated with different weld quality characteristics in butt welding. The RMS value of arc power was found to be strongly correlated with joint tensile strength (7-8). So, RMS value of current and voltage were further used to develop the process modelling. These sensors' signals have also been further analyzed in time-frequency wavelet mode to measure the higher level wavelet packet coefficients which were further used to improve the prediction capability of the models

2. Time-frequency Wavelet Analysis

The wavelet transform is localized in both time and frequency instead of only frequency as in case of Fourier transform. Wavelet analysis is an efficient windowing technique with variable sized windows. It allows the use of long time intervals for low frequency information and shorter regions for high frequency information. Thus, it can analyze the localized high frequency area of a larger signal.

The wavelet is a mathematical function used to divide a continuous mode time function (or signal) into different scale components. The wavelet transform represents a signal by wavelets, which contains translated and scaled wave functions of a finite length wave, called as mother wavelet. Generally, a wavelet is expressed mathematically as:

$$W_{ab}(t) = \frac{1}{\sqrt{|a|}} W\left(\frac{t-b}{a}\right) \tag{1}$$

where, b indicates location parameter and a stands for scaling parameter [9].

The wavelet transfer function may be expressed as:

$$C(a,b) = \int_t f(t).\frac{1}{\sqrt{|a|}} W\left(\frac{t-b}{a}\right).dt \tag{2}$$

For every (a, b) interval, it shows a wavelet transform coefficient which represents the degree of similarity of the scaled wavelet to the function at the position of *t = (b/a)*. A critical sampling indicates the resolution of discrete wavelet transform (DWT) in both time and frequency. It shows minimum number of wavelet packet coefficients sampled from continuous wavelet transform (CWT), which ensure about all the information present in the original signal. In critical sampling $a=2^{-j}$ and $b=k.2^{-j}$, where integer j and k represent the discrete translation and discrete dilations, respectively. Then *C (a, b)* can be expressed as *C (j, k).*

$$C(j,k) = \int_t f(t).2^{j/2}.W(2^j t - k)dt = \int_t f(t).W_{j,k}(t) \tag{3}$$

In the wavelet packet analysis, the original signal *W (0, 0)* has been decomposed into two separate frequency band part as low frequency and high frequency component by passing the signal through a high-pass and low-pass filter, respectively in the first level of decomposition. This decomposition process will be continued up to the number of level of decomposition under consideration. In this work, original signal W (0, 0) have been decomposed into three levels which is represented by tree structures as shown in Fig. 2. 1-D wavelet packet decomposition has been carried out using MATLAB 7.8. The signal features has found to be insignificant at higher levels beyond this third level of decomposition. The RMS values of the third level wavelet packet function $W(j,k)_{j\in[0,3];k\in[0,7]}$ are termed as $C(j,k)_{j\in[0,3];k\in[0,7]}$, which have been processed related to the frequency band under consideration.

In this work, these wavelet coefficients corresponding to third level of decomposition were assumed as C (3,0) for frequency band of 0Hz to 2500Hz, C (3,1) for 2500 to 5000 and so on up to C (3,7) for 17500Hz to 20000Hz, where sampling rate was 40 kHz. The Daubechies family of wavelets *(dbM)* has been considered, where M indicates the order of mother wavelet function.

Sensitivity analysis has been carried out to identify significant wavelet coefficients of voltage and current signals. The most significant wavelet packet coefficients for voltage [V(3,0), V(3,4), V(3,6)] and current signals [(I(3,1), I(3,3), I(3,4)] of the welding experiments (53 experiments for the model development and 7 more experiments for validation of models) along with RMS value of voltage and current signals and weld quality features are shown in Table 1

Table 1: Process parameters with corresponding sensors' outputs and joint features

	Process parameters						*RMS V& I*		*Significant wavelet packet coefficients*						*Joint features*	
Sl. no	*F*	*S*	a_t	*Vp*	*fp*	*tp*	*Vr*	*Ir*	*I(3,1)*	*I(3,3)*	*I(3,4)*	*V(3,0)*	*V(3,4)*	*V(3,6)*	*ΔHw-h*	σ_t
1	7	5.8	-15	30.4	144	4.6	24.3	216	0.054	0.029	0.015	0.93	0.013	0.028	85	3531
2	8	5.8	-15	35.4	144	4.6	26.1	259	0.051	0.026	0.014	0.99	0.007	0.019	23	5137
3	8	5.8	-15	30.4	144	3.4	20.3	239	0.092	0.054	0.025	2.04	0.020	0.042	83	3402
4	8	5.8	-15	35.6	105	3.4	21.9	240	0.065	0.034	0.020	1.79	0.019	0.042	94	280.2
5	7	5.8	-15	35.6	105	3.4	24.1	231	0.052	0.027	0.016	1.28	0.008	0.020	68	483.2
6	7	5.8	-15	35.6	105	4.6	23.9	231	0.047	0.026	0.016	1.38	0.008	0.021	30	507.6
7	8	5.8	-15	30.4	105	4.6	20.6	236	0.080	0.043	0.022	1.79	0.021	0.043	93	336.3
8	7	5.8	-15	30.4	105	3.4	19.4	217	0.081	0.045	0.024	1.70	0.018	0.040	87	383.7
9	8	8.8	-15	30.4	144	4.6	22.9	236	0.072	0.039	0.019	1.54	0.020	0.043	83	346.7
10	8	8.8	-15	35.6	144	3.4	23.7	246	0.058	0.029	0.017	1.45	0.016	0.034	94	363.9
11	7	8.8	-15	35.6	105	3.4	21.9	221	0.052	0.028	0.019	1.51	0.017	0.037	85	368.3
12	8	8.8	-15	30.4	105	3.4	18.2	237	0.096	0.055	0.028	1.89	0.019	0.039	98	130.7
13	7	8.8	-15	30.4	105	4.6	20.6	213	0.080	0.045	0.023	1.70	0.017	0.037	73	491.7
14	8	8.8	-15	35.6	105	4.6	23.5	253	0.052	0.028	0.017	1.47	0.015	0.033	28	223.6
1	7	8.8	-15	30.4	1	3	2	2	0	0	0	1	0	0	8	4

International Research Journal of Engineering and Technology (IRJET) e-ISSN: 2395-0056
Volume: 04 Issue: 08 | Aug -2017 www.irjet.net p-ISSN: 2395-0072

5					44	.4		0.6	16		.076	.043	.022	.61	.017	.033		5	37.4
16	7	8.8	-15	35.6	144	4.6		26.4	238		0.050	0.027	0.013	0.96	0.007	0.037		54	373.7
17	7	5.8	15	35.6	105	3.4		23.3	220		0.070	0.039	0.021	1.90	0.022	0.021		81	416.2
18	8	5.8	15	35.6	105	4.6		24.3	244		0.059	0.032	0.018	1.65	0.021	0.046		70	315.1
19	7	5.8	15	30.4	144	3.4		21.4	219		0.083	0.049	0.023	1.94	0.023	0.045		51	506.7
20	7	5.8	15	30.4	105	4.6		22.1	215		0.076	0.045	0.021	1.87	0.007	0.041		74	384.9
21	8	5.8	15	35.6	144	3.4		25	243		0.076	0.041	0.020	1.93	0.020	0.043		31	137.8
22	7	5.8	15	35.6	144	4.6		27	238		0.050	0.026	0.013	0.90	0.024	0.048		60	347.7
23	8	5.8	15	30.4	105	3.4		19.9	240		0.099	0.061	0.028	2.14	0.020	0.021		117	401.7
24	8	5.8	15	30.4	144	4.6		23.8	237		0.081	0.043	0.020	1.95	0.007	0.041		117	399.1
25	8	8.8	15	30.4	144	3.4		20.3	239		0.098	0.057	0.027	2.09	0.018	0.049		61	352.5
26	7	8.8	15	35.6	144	3.4		25.4	232		0.054	0.027	0.016	1.21	0.024	0.042		65	288
27	7	8.8	15	30.4	105	3.4		18.7	219		0.091	0.054	0.026	1.81	0.006	0.020		43	380
28	7	8.8	15	30.4	144	4.6		24.5	218		0.061	0.033	0.016	2.67	0.007	0.039		85	520
29	7	8.8	15	35.6	105	4.6		23.8	236		0.049	0.026	0.016	1.29	0.020	0.050		90	354.4
30	8	8.8	15	35.6	144	4.6		25.8	264		0.052	0.027	0.014	1.02	0.020	0.020		77	244.7
31	8	8.8	15	35.6	105	3.4		22.6	240		0.068	0.037	0.021	1.71	0.017	0.020		21	410.3
32	8	8.8	-35	30.4	105	4.6		20.6	241		0.078	0.044	0.022	1.71	0.023	0.043		84	400.3
33	8	7.7	35	33	124	4		22.5	242		0.058	0.032	0.018	1.32	0.020	0.038		83	404
34	8	7.7	0	33	124	4		23.4	242		0.085	0.048	0.023	1.89	0.014	0.046		36	368.9
35	8	7.7	0	33	124	4		22.7	228		0.062	0.033	0.018	1.54	0.019	0.044		68	421.4
36	8	9.9	0	33	124	4		22.4	229		0.052	0.028	0.017	1.26	0.023	0.033		65	225
37	8	7.7	0	33	124	4		22.6	227		0.056	0.030	0.017	1.36	0.020	0.042		95	399.9
38	8	4.6	0	33	124	4		23.9	231		0.075	0.045	0.020	2.18	0.021	0.047		59	411.3
39	8	7.7	0	33	124	4		22.9	225		0.062	0.033	0.018	1.53	0.022	0.044		80	403.2
40	8	7.7	0	33	124	4		22.9	226		0.063	0.033	0.018	1.57	0.009	0.046		62	452.9
41	8	7.7	0	33	124	4		23.8	226		0.071	0.040	0.019	1.93	0.022	0.047		65	475.9
42	8	7.7	0	33	124	4		25.8	233		0.054	0.028	0.013	0.89	0.009	0.023		71	373.5

43	8	7.7	0	27	124	4		20.4	226		0.089	0.054	0.026	2.31	0.036	0.053		54	130.4
44	8	7.7	0	39	124	4		27.8	252		0.050	0.025	0.017	1.49	0.009	0.021		131	187
45	8	7.7	0	39	80	4		19.5	226		0.068	0.037	0.022	1.73	0.018	0.038		82	499
46	8	7.7	0	33	124	2.6		19.9	227		0.095	0.055	0.027	0.22	0.021	0.044		105	397.8
47	8	7.7	0	33	124	5.4		24.4	234		0.048	0.026	0.012	0.03	0.006	0.019		95	272.1
48	8	7.7	0	33	124	4		23.7	227		0.069	0.037	0.019	0.24	0.021	0.047		25	337.2
49	6	7.7	0	33	124	4		23.8	204		0.0.55	0.031	0.016	0.14	0.015	0.034		66	419.1
50	9	7.7	0	33	124	4		23.2	251		0.073	0.039	0.020	0.23	0.021	0.045		87	409.3
51	8	7.7	0	33	124	4		22.4	231		0.058	0.032	0.018	0.21	0.018	0.041		79	416.3
52	8	7.7	0	33	124	4		23	227		0.067	0.035	0.018	0.22	0.021	0.043		68	409.3
53	8	7.7	0	33	124	4		23.1	225		0.065	0.034	0.018	0.22	0.020	0.042		73	416.3
54	7	7.2	0	33	84	4.2		19.2	221		0.083	0.050	0.018	0.19	0.022	0.041		113	136
55	8	7.6	-25	28	121	3.8		18.8	236		0.099	0.051	0.021	0.21	0.028	0.049		95	283.2
56	8	8	-15	36	136	4.5		25.2	239		0.052	0.027	0.012	0.23	0.021	0.030		53	451.3
57	7	6.8	-25	32	92	4		22.4	217		0.064	0.031	0.017	0.20	0.023	0.041		71	323
58	8	7.6	-15	34	124	3.2		23.7	220		0.061	0.034	0.013	0.22	0.031	0.047		54	387.1
59	7	7.2	25	38	112	3.6		24.3	219		0.053	0.042	0.011	0.14	0.017	0.021		47	417.2
60	8	7.6	15	35	100	4.6		25.5	241		0.056	0.030	0.011	0.19	0.023	0.030		71	332.1

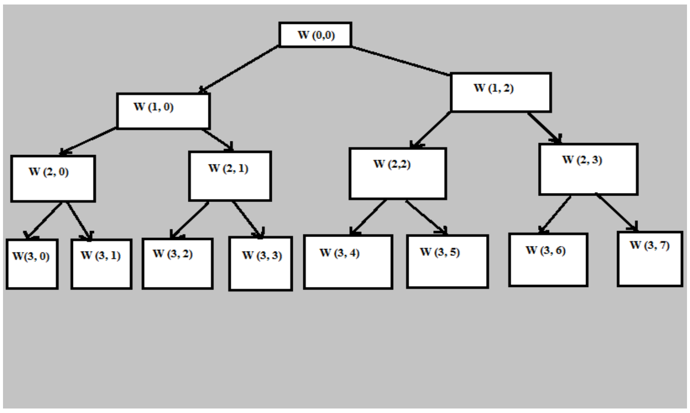

Fig.2. Wavelet packet tree for third level decomposition of acquired sensors' signals

3. Development of RSM and ANN model

Response surface is a functional mapping of multiple process parameters to a single output feature. In the present research, second order polynomial response surface models are developed using first 53 sets of data to correlate six input process parameters: *S*, *F*, α_t, V_p f_p, and t_p with the each weld quality feature. The MINITAB (release 13.31, Minitab Inc. 2002) software was used for the model development and further statistical analysis to check the adequacy of the model. The hardness variation from WZ to HAZ (ΔH_{w-h}) and joint ultimate tensile strength (σ_t) were modelled as joint quality features as shown in equation 4 and 5. The adequacy of the models was tested with 95% confidence level using the analysis of variance (ANOVA) technique. When the calculated value of 't' corresponding to a coefficient exceeds the standard tabulated value, the coefficient may be considered as significant. The significant regression coefficients were recalculated to develop the final model. Finally, the adequacy of the models was tested with 95% confidence level using the analysis of variance (ANOVA) technique

$$\Delta H_{w-h} = -101.5 + 0.3\alpha_t - 16.37S + 113.3F - 31.9V_p + 215t_p + 1.5s^2 + 3.3F^2 + 0.9V_p^2 - 7t_p^2$$
$$-0.2\alpha_t F + 0.7\alpha_t t_p - 2.2SF + 0.2SV_p + 0.1Sf_p - St_p - 1.8FV_p - 0.3Ff_p - 12.1Ft_p - 3.8V_p t_p + 0.4 f_p t_p \quad (4)$$

$$\alpha_t = 697.2 - 0.4\alpha_t - 135.2S - 595F + 177.1V_p + 2.8 f_p + 545.9t_p - 5S_2 + 17.9F^2 + 3.9V_p^2 + 0.7\alpha_t S + 0.7\alpha_t F - 0.2\alpha_t V_p - 2.7\alpha_t t_p$$
$$+15.3SF + 19.SV_p - 0.2Sf_p + 10St_p + 8.4FV_p + 2.1Ff_p + 56.8Ft_p - 0.1V_p f_p + 8.1V_p t_p - 1.6 f_p t_p \quad (5)$$

The multi-layered feed-forward network with back propagation gradient descent learning algorithm is widely used in welding process modelling. The feed forward network constitutes an input layer, an output layer and any number of hidden layers. Each layer is comprised of a variable number of nodes as neurons. In the present work, a code for multi-neuron, multi-layered back-propagation (BPNN) model is used for mapping the P-MIGW process parameters to weld quality characteristics.

In this work single hidden layer with log-sigmoidal transfer function (*f*) has been used in all the layers considering the non-linearity of the process behaviour. The nodes of each layer are interconnected to the preceding and subsequent layer nodes with synaptic weights. In the forward pass, the weighted inputs (*I*) are summed up to determine the output (*O*) of the neuron as per equation 6. The weight of each preceding nodes (w_{ji}) multiplied by corresponding inputs (y_i) whose summed up value indicate the weighted input of j^{th} neuron.

$$O = f(I) = f\left(\sum w_{ji} y_i\right) \quad (6)$$

Training algorithms change the inter-neuron weights in such a way as to reduce a desired error function (*E*) relating the target values (T_i) to the actual output (O_i) values (equation 7).

$$E = \frac{1}{N}\sum_{1}^{N}\left(T_i - O_i\right)^2 \quad (7)$$

Each synaptic weight is modified from W_{old} to W_{new} according to an error correction rule (equation 3) based on the gradient descent technique to minimize the mean square error (MSE) between actual p^{th} output (O_{pk}) and desired p^{th} output (T_{pk}) to the total number of training pattern (*N*) during the backward pass as per equation 8. The learning rate (η) is to be adjusted to reduce MSE. The momentum coefficient (α) has also been used to maintain the stability of η with adequate learning according to delta rule.

$$W_{new} = W_{old} - \eta \frac{\partial E}{\partial W_i} \quad (8)$$

$$MSE = \frac{1}{2N}\sum_{k=1}^{N}\sum_{p=1}^{P}\left(T_p^k - O_p^k\right)^2 \quad (9)$$

The performance of the model depends on the network parameters like number of neurons in hidden layer (*j*), no of hidden layer (*h*), learning rate of the synaptic weights (η) and momentum coefficient (α). There is no significant improvement of MSE in testing with the consideration of more number of hidden layers in the present case. Thus, single hidden layer is considered, whereas *j*, η and α were varied from 1 to 30, 0.1 to 0.9 and 0.1 to 0.9, respectively. Single hidden layer was found to be sufficient to reduce MSE in training as well as testing with less number of iterations (i.e. less computational time). Several trials were made to finally obtain the optimal architecture, which can provide the minimum MSE in testing. The optimum architecture was found by varying the number of neurons in the hidden layer along with the variation of η and α. This evaluation was carried out by the determination of MSE in testing (MSE_TEST) based on the absolute prediction error value of the weld quality characteristics.

The RMS value of arc current and voltage were used with process parameters in BPNN models to improve the prediction capability as RMS arc power was found to be correlated with joint mechanical properties. Various combinations of sensors' signal features were used along with six process parameters to investigate the weld quality prediction as shown in Table 2. The process parameters were only been considered in Strategy #1. The

RMS value of welding signals (current and voltage) was used in Strategy #2. Wavelet packet coefficients of current and voltage signal with process parameters were used in Strategy #3 and #4, respectively. Finally, the best wavelet packet coefficients of the voltage and current signals were considered in Strategy #5.The number of neurons in the input layer of the developed BPNN models depends on the strategy under consideration.

Table 2. Weld quality prediction strategies

Sl no	Features used in the BPNN model	Number of input nodes
1	Six process parameters	6
2	Six process parameters with RMS welding	8
3	Six parameters with RMS values of wavelet packet coefficients of current signa	14
4	Six parameters with RMS values of wavelet packet coefficients of voltage signal	14
5	Six parameters with RMS values of significant wavelet packet coefficients of current and voltage signals	16

4. Result and Discussions

The ANOVA results are shown in Table 3 and Table 4 for two weld quality feature models. The acceptance of these models mainly depends on P-value, F-value and R^2 value. P-value indicates the probability of significance. It is calculated based on the F-ratio. The P-value is then compared with the assumed confidence level (in this case 95 %). If the P-value is less than 0.05, then the model may be accepted. The F-value of the model has to be higher than the tabulated F- value at 95 % confidence level at respective DOF of both the regression model and residual error. Thus, these criteria were found to be fulfilled, i.e. the regression models were acceptable. However, the R^2 value i.e. the coefficient of correlation indicates the closeness of the predicted output values with the actual experimental responses. Its' value lies in between 0 to 1. Higher R^2 value indicates better model. The R^2 values for hardness variation ($\Delta H_{w\text{-}h}$) and tensile strength (σ_t) were found to be less than 0.85. Thus, the mean absolute prediction errors for seven validation experiments were found to be more than 35% (Table 6). Therefore, it may be concluded that the second order regression equations are not so adequate to represent the relationship between process parameters with respect to these two weld quality characteristics.

Table 3. ANOVA table for hardness variation ($\Delta H_{w\text{-}h}$) model

Source	DOF	SS	MS	F-value	P-value
Equation 4	26	24465.8	940.99	5.89	0.000
Residual error	26	4153.5	159.75		
Total	52				

$F_{0.05,\,26,\,26} = 1.94$

Table 4. ANOVA table for joint tensile strength (σ_t) model

Source	DOF	SS	MS	F-value	P-value
Equation 5	26	450447	17324.9	4.10	0.000
Residual error	26	109801	4223.1		
Total	52	560248			

$F_{0.05,26,26} = 1.94$

The simulation result of various strategies using BPNN code was compared according to prediction error (Table 5). The prediction capability of the various neural network structures were compared with mean square error in testing (MSE_TEST). The 6-30-2 architecture with η and α as 0.4, and 0.4, respectively proved the best data fitting for the prediction of joint tensile strength and hardness variation without considering sensor features. This optimum architecture provided the minimum MSE in training (MSE_TRAIN) and testing (MSE_TEST) as 0.007358 and 0.009317, respectively.

Table 5. Prediction performance of BPNN models for weld quality features using various strategies

Process outputs	Strategy No	Best Network	Optimum η	Optimum α	MSE_TRAIN	MSE_TEST
Σt, $\Delta H_{w\text{-}h}$	1	6-30-2	0.4	0.4	0.007358	0.009317
	2	8-29-2	0.5	0.4	0.009733	0.007742
	3	14-4-2	0.5	0.1	0.002864	0.005781
	4	14-4-2	0.6	0.5	0.003861	0.007341
	5	16-12-2	0.5	0.5	0.004917	0.006355

The absolute prediction error was found to be 14.69% and 27.18% for joint tensile strength and hardness variation, respectively. However, joint strength prediction error was considerably reduced to 7.44% considering best sensor based strategy (strategy #3) as shown in Table 6. The 14-4-2 network structure with learning rate and momentum coefficient of 0.5 and 0.1, respectively, was found as the best network parameters for the prediction of joint strength and hardness variation at the interface of weld fusion zone to unaffected base plate. The minimum MSE in training (MSE_TRAIN) and testing (MSE_TEST) using this best network were 0.002864 and 0.005781, respectively. Therefore, it may be concluded that wavelet feature of current signal is an important indicator to monitor joint strength.

Table 6. Comparison of prediction performance of various modelling techniques

Weld quality Features	Mean absolute prediction error (%) using		
	RSM	BPNN	Sensor based BPNN (Strategy #3)
ΔHw-h	36.90	14.69	14.86
	37.45	27.18	7.44

The actual joint tensile strength of the seven validation experiments with predicted values using RSM, BPNN and best sensor based BPNN (Strategy #3) are shown in Fig 3. The predicted value of individual tests using sensor based BPNN technique were almost close to experimental values. Therefore, sensor based features are highly useful to predict weld quality features in a better way.

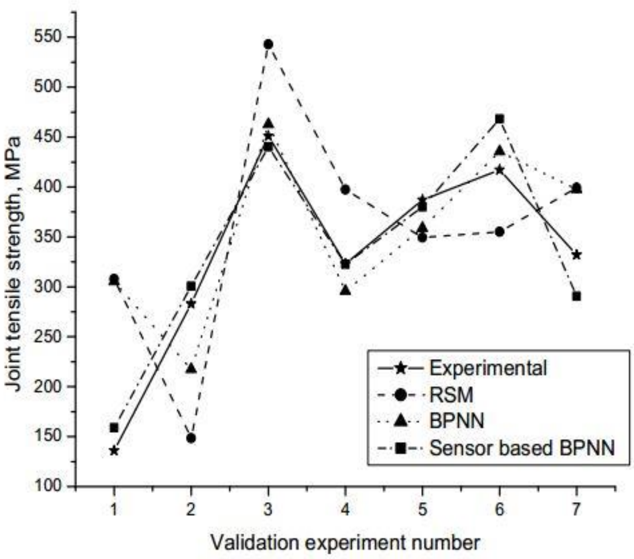

Fig. 3. Prediction of joint tensile strength using various modelling techniques

5. Conclusion

The arc sensors' signals are strongly correlated with joint mechanical properties in P-MIGW process. The mathematical regression model is inadequate to predict weld joint strength. However, it is significantly improved using wavelet packet coefficients of current signal in back-propagation ANN technique. The average prediction error was reduced from 37% using RSM model to 21% using BPNN models which again further improved to 11% using wavelet features of current signal with six process parameters which is highly competitive with earlier works. Thus, BPNN models are better than response surface regression models in terms of prediction capability. The current signal wavelet values are highly useful to improve joint strength monitoring capability.

References

[1]. I.E. French, and M.R. Bosworth, "A comparison of pulsed and conventional welding with basic flux cored and metal cored welding wires", Welding Journal, Vol.74, Issue 6, 1995, pp. 197s–205s.
[2]. K. Stanzel, "Pulsed GMAW cuts cycle time by 600 percent", Welding Design and Fabrication, 2001,pp. 85–87.
[3]. E. Karadeniz, , U. Ozsarac, and C. Yildiz, "The effect of process parameters on penetration in gas metal arc welding processes", Material Design, Vol. 28, Issue 2, 2007, pp. 649–656.
[4]. G. Powell, and G. Herfurth, "Charpy V-notch properties and microstructures of narrow gap ferritic welds of a quenched and tempered steel plate", Metallur. Mater. Trans. A, Vol. 29, Issue 11, 1998, pp. 2775-2784.
[5]. Y.M. Zhang, E. Liguo, and B.L. Walcott, "Robust control of pulsed gas metal arc welding", J. Dyn. Syst. ,Meas. Contr., ASME, Vol. 124, 2000, pp. 1–9.
[6]. H.C.D. Miranda, A. Scotti and V.A. Ferraresi, "Identification and control of metal transfer in pulsed GMAW using optical sensor", Sci. Tech. Weld. Join., Vol. 12, Issue 3, 2007, pp. 249-257.
[7]. K. Pal, S. Bhattacharya, and S.K. Pal, "Investigation on arc sound and metal transfer modes for on-line monitoring in pulsed gas metal arc welding", Journal of Materials Processing Technology, Vol.210, Issue 10, 2010, pp. 1397-1410.
[8]. K. Pal and S.K. Pal, "Monitoring of weld penetration using arc acoustics in pulsed MIG welding", Materials and Manufacturing Processes, Vol. 26, 2011, pp. 684-693.
[9]. K.P. Soman and K.I. Ramachandran, "Insight into wavelets from theory to practice", Prentice-hall Ind. Pvt. Ltd., 2nd edition., 2006.